Supplemental Material can be found at:
http://www.jbc.org/content/suppl/2012/05/01/M112.359547.DC1.html

⌘ *Author's Choice*

THE JOURNAL OF BIOLOGICAL CHEMISTRY VOL. 287, NO. 25, pp. 20823–20829, June 15, 2012
© 2012 by The American Society for Biochemistry and Molecular Biology, Inc. Published in the U.S.A.

Structural Analysis of SHARPIN, a Subunit of a Large Multi-protein E3 Ubiquitin Ligase, Reveals a Novel Dimerization Function for the Pleckstrin Homology Superfold*[S]

Received for publication, March 6, 2012, and in revised form, April 17, 2012 Published, JBC Papers in Press, May 1, 2012, DOI 10.1074/jbc.M112.359547

Benjamin Stieglitz[‡], Lesley F. Haire[‡], Ivan Dikic[§], and Katrin Rittinger[‡1]

From the [‡]Division of Molecular Structure, Medical Research Council National Institute for Medical Research, The Ridgeway, London NW7 1AA, United Kingdom and the [§]Buchmann Institute for Molecular Life Sciences and Institute of Biochemistry II, Goethe University School of Medicine, D-60590 Frankfurt, Germany

Background: SHARPIN is a subunit of the E3 ligase complex LUBAC and the gene that is mutated in chronic proliferative dermatitis mice.
Results: The N-terminal portion of SHARPIN adopts the PH superfold and mediates homodimerization.
Conclusion: The PH superfold can be used as a protein dimerization module.
Significance: This study highlights the versatility of the PH superfold and its function as a protein interaction module.

SHARPIN (SHANK-associated RH domain interacting protein) is part of a large multi-protein E3 ubiquitin ligase complex called LUBAC (linear ubiquitin chain assembly complex), which catalyzes the formation of linear ubiquitin chains and regulates immune and apoptopic signaling pathways. The C-terminal half of SHARPIN contains ubiquitin-like domain and Npl4-zinc finger domains that mediate the interaction with the LUBAC subunit HOIP and ubiquitin, respectively. In contrast, the N-terminal region does not show any homology with known protein interaction domains but has been suggested to be responsible for self-association of SHARPIN, presumably via a coiled-coil region. We have determined the crystal structure of the N-terminal portion of SHARPIN, which adopts the highly conserved pleckstrin homology superfold that is often used as a scaffold to create protein interaction modules. We show that in SHARPIN, this domain does not appear to be used as a ligand recognition domain because it lacks many of the surface properties that are present in other pleckstrin homology fold-based interaction modules. Instead, it acts as a dimerization module extending the functional applications of this superfold.

SHARPIN (also known as Sipl1) is a 387-amino acid protein that originally has been identified as a SHANK (SH3 (Src homology 3) and multiple ankyrin repeat domains protein)-binding protein enriched in the postsynaptic density of excitatory neurotransmitters (1). More recently, the observation that a spontaneous mutation in the mouse SHARPIN gene causes chronic proliferative dermatitis, a disease marked by skin lesions, multi-organ inflammation, and a deficient immune system suggested that SHARPIN might also be implicated in immune and inflammatory signaling pathways (2). Such a role has now been confirmed by the discovery that SHARPIN acts as a novel subunit of the E3 ubiquitin ligase complex LUBAC, which catalyzes the formation of linear or M1-linked polyubiquitin chains that play an important role in the activation of the transcription factor NF-κB (3–5). LUBAC contains two other subunits, termed HOIL-1L (also known as RBCK1) and HOIP (HOIL-1L interacting protein, also known as RNF31), both of which are members of the RBR (RING-between-RING) subfamily of RING family E3 ligases (6), with the RBR domain residing in the C-terminal portion of the molecules (7–10). The N-terminal half of HOIL-1L consists of an ubiquitin-like domain (UBL)[2] followed by an Npl4 zinc finger (NZF). The UBL recognizes an ubiquitin-associated domain in HOIP to mediate complex formation (7).

Other domains present in HOIP include a PUB (Peptide: *N*-glycanase/UBA or UBX-containing proteins) domain followed by a zinc finger (ZF) and two NZF domains. Mutational studies have shown that the RBR domain of HOIP is the active side for linear ubiquitin chain synthesis, whereas the RBR of HOIL-1L is dispensable for catalysis, although complex formation between the two proteins is required for enzymatic activity (7, 8). SHARPIN does not contain an RBR domain but shares significant similarity with the N-terminal region of HOIL-1L that comprises the UBL and NZF domains (see Fig. 1*A*) and similar to HOIL-1L binds ubiquitin via the NZF, whereas its UBL domain is responsible for the interaction with HOIP (3–5). This related domain architecture and sequence similarity likely explains the apparent overlapping function of the two proteins as SHARPIN can substitute for HOIL-1L in promoting linear ubiquitin chain synthesis by HOIP. Furthermore, the observation that endogenous HOIP can form a complex with only

* This work was supported by Medical Research Council UK Grant U117565398.
⌘ *Author's Choice*—Final version full access.
The atomic coordinates and structure factors (code 4EMO) have been deposited in the Protein Data Bank, Research Collaboratory for Structural Bioinformatics, Rutgers University, New Brunswick, NJ (http://www.rcsb.org/).
[S] This article contains supplemental Figs. S1–S4 and an additional reference.
[1] To whom correspondence should be addressed: Div. of Molecular Structure, MRC-National Institute for Medical Research, The Ridgeway, London NW7 1AA, UK. Tel.: 44-20-88162395; Fax: 44-20-8816580; E-mail: katrin.rittinger@nimr.mrc.ac.uk.

[2] The abbreviations used are: UBL, ubiquitin-like domain; NZF, Npl4-zinc finger; TCEP, tris(2-carboxyethyl)phosphine; MALS, multi-angle laser light scattering; ITC, isothermal titration calorimetry; AUC, analytical ultracentrifugation.

Downloaded from www.jbc.org at Frankfurt University Library / Section Bibliothek Naturwissenschaften, on August 31, 2012

HOIL-1L or SHARPIN in the absence of the other and that either of these complexes can synthesize linear ubiquitin chains to promote NF-κB activation indicates that some of the functions of the two proteins are redundant (3, 5, 8). Nevertheless, clear functional differences exist: it has been shown that SHARPIN but not HOIL-1L deficiency in mice results in an increased TNFα-induced cell death, whereas HOIL-1L has a much more profound effect on IL-1β-induced NF-κB activation (3–5). These specific functions of SHARPIN and HOIL-1L are most likely mediated by distinct structural features outside the UBL-NZF segment that is shared between the two proteins. SHARPIN contains a 170-amino acid stretch at the N terminus, which is not well characterized and is absent in HOIL-1L. Immune precipitation experiments showed this region to undergo homomultimerization, an observation that is in line with the presence of a short heptad repeat motif-spanning residues 36–49 that is predicted to form a coiled coil (1). However, apart from these findings, no further information about the functional or structural properties of the N-terminal part of SHARPIN is currently available. To gain insight into the properties of this region, we have solved the x-ray structure of a SHARPIN construct containing residues 1–127 and characterized its propensity for self-association. The structure confirms that SHARPIN has the ability to self-associate into dimers but rather unexpectedly shows that dimerization is not mediated by a coiled coil but that SHARPIN utilizes the pleckstrin homology (PH) superfold as a dimerization module instead. This mode of interaction is unique and represents a novel function for the PH superfold.

EXPERIMENTAL PROCEDURES

Cloning, Expression, and Purification—The N-terminal fragment of human SHARPIN comprising residues 1–127 was expressed in pGEX-4T1 (GE Healthcare). The interface mutant V114D and the mutant L22M/L101M used for producing selenomethionine-substituted protein was generated by site-directed mutagenesis according to the QuikChange protocol (Stratagene) and verified by DNA sequencing. The protein was purified on GSH-Sepharose, and the GST was cleaved with thrombin at 4 °C overnight. The cleaved protein was further purified by gel filtration using a Superdex S75 column (GE Healthcare) run in 50 mM HEPES, pH 7.4, 150 mM NaCl, and 1 mM DTT. Purified SHARPIN was concentrated to a final concentration of 5 mM and stored at −80 °C.

Crystallography—Crystallization of SHARPIN 1–127 and SHARPIN 1–127 L22M/L101M will be described in detail elsewhere. In brief, crystals were grown from a 10 mg/ml protein solution in sitting drop set-ups using a reservoir solution containing 4 M sodium formate and optimized by seeding. The mother liquor was not buffered, and its pH was measured to be pH 7.7. Crystals were flash-frozen in liquid nitrogen with a solution containing the mother liquor and 10% glycerol. Data were collected at 100 K. Crystals diffract to 2.0 Å and belong to the primitive tetragonal space group $P4_32_12$ with four molecules per asymmetric unit. A data set of high redundancy was collected on beamline I0.4 at the Diamond Light Source (Oxford, UK) and processed using Denzo and Scalepack (11). The structure was solved by single anomalous dispersion phasing using the SeMet derivative SHARPIN 1–127 L22M/L101M. Heavy atom search, density modification, and initial model building was performed using Phenix AutoSol (12). After several rounds of iterative manual model building with Coot (13), the structure was refined using the program REFMAC5 (14), and the stereochemistry of the final model was analyzed with Procheck (15).

Isothermal Titration Calorimetry—Dilution experiments were conducted to investigate the dissociation process of the monomer-dimer transition using an ITC200 calorimeter (GE Healthcare). Protein samples of WT and mutant V114D SHARPIN were prepared by dialysis against 50 mM HEPES, pH 7.4, 150 mM NaCl, 1 mM tris(2-carboxyethyl)phosphine (TCEP)). Measurements were performed at 25 °C, and data were analyzed using the Origin-based software provided by the manufacturer.

Analytical Ultracentrifugation—Sedimentation velocity experiments were performed in a Beckman Optima XL-I analytical ultracentrifuge using conventional aluminum double-sector centerpieces and quartz windows. Solvent density, viscosity, and the protein partial specific volumes were calculated using SEDNTERP. Prior to centrifugation, samples were prepared by dialysis against the buffer blank solution, 50 mM HEPES, pH 7.4, 150 mM NaCl, and 1 mM TCEP. Samples (400 μl) and buffer blanks (420 μl) were loaded into the cells, and centrifugation was performed at 50,000 rpm and 293 K in an An-60 Ti rotor. Interference images were collected every 180 s during the sedimentation run. The data were analyzed as a distribution of sedimentation coefficients using SEDFIT (16). Sedimentation equilibrium experiments were performed in a Beckman Optima XLA analytical ultracentrifuge using charcoal-filled epon six-channel centerpieces in an An-60 Ti rotor. Prior to centrifugation, samples were prepared by dialysis against the buffer blank solution, 50 mM HEPES, pH 7.4, 150 mM NaCl, and 1 mM TCEP. The solutions were allowed to reach equilibrium at 18,000, 20,000, 26,000, and 30,000 rpm. To determine the dissociation constant (K_d), the sedimentation equilibrium data were fitted globally with the programm SEDPHAT (17) using a monomer-dimer ideal solution model.

Multi-angle Laser Light Scattering (MALS)—Molecular mass and molecular mass distributions were determined using size exclusion chromatography coupled to multi-angle light scattering. Samples of WT and mutant V114D SHARPIN were applied in a volume of 100 μl to a Superdex 75 10/300 GL column (GE Healthcare) equilibrated in 50 mM HEPES, pH 7.4, 150 mM NaCl, and 1 mM TCEP, at a flow rate of 0.5 ml/min. The column was mounted on a Jasco HPLC. The scattered light intensity of the column eluate was recorded using a DAWN-HELEOS laser photometer (Wyatt Technology, Santa Barbara, CA). The protein concentration of the eluent was determined using an OPTILAB-rEX differential refractometer (Wyatt Technology). The weight-averaged molecular mass of the eluent was determined using the ASTRA software (version 5.1; Wyatt Technology). Measurements were performed at 25 °C.

RESULTS AND DISCUSSION

Self-association of N-terminal Portion of SHARPIN—SHARPIN contains 387 amino acids with UBL and NZF

Downloaded from www.jbc.org at Frankfurt University Library / Section Bibliothek Naturwissenschaften, on August 31, 2012

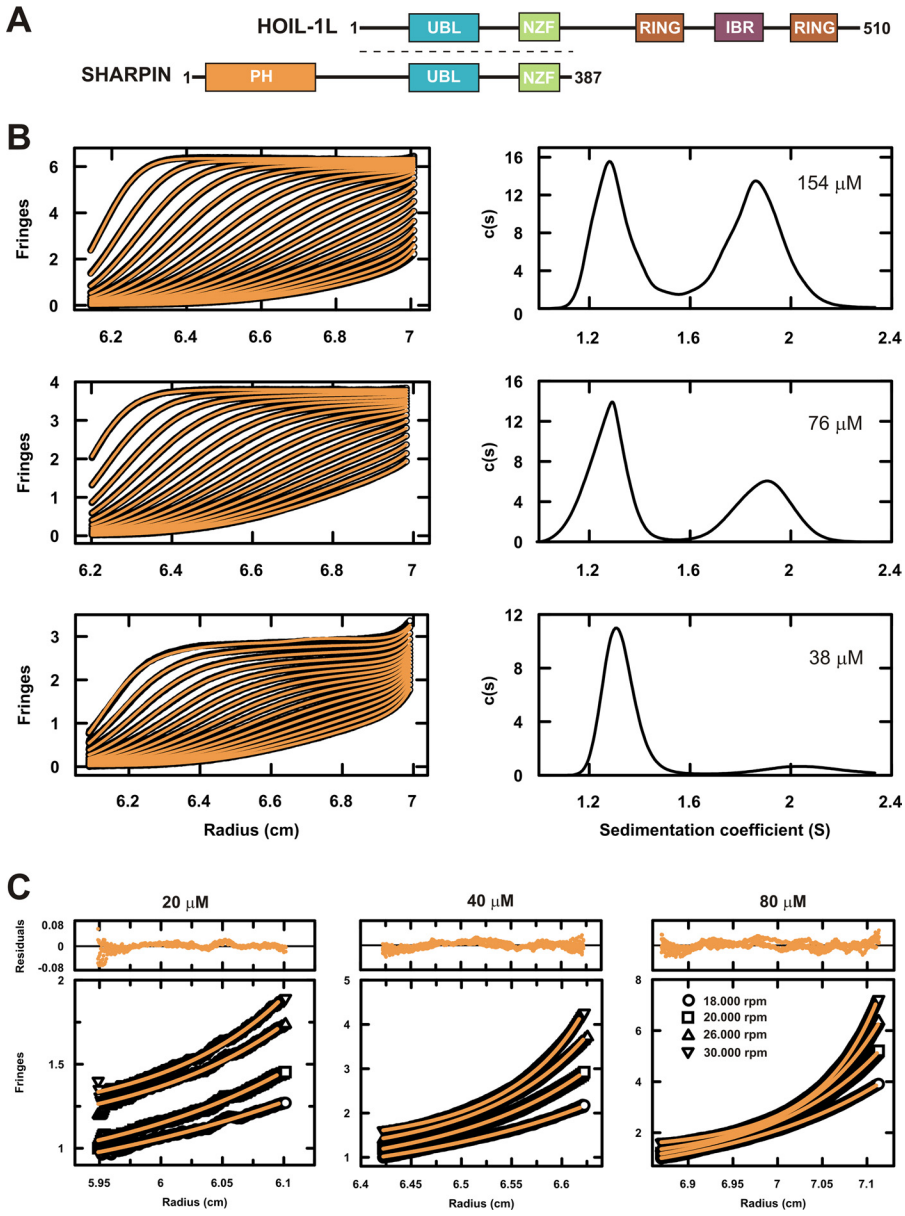

FIGURE 1. *A*, schematic drawing of the domain organization of HOIL-1L and SHARPIN. The *dashed line* indicates the region of sequence similarity (*RING*, really interesting new gene; *IBR*, in-between-ring). *B*, sedimentation velocity size distribution analysis of SHARPIN 1–127 at three different concentrations (38, 76, and 154 μM). The fitted boundary scans are shown in the *left panels* and the corresponding *c*(*s*) analyses are shown in the *right panels*. *C*, sedimentation equilibrium traces with residual plots for SHARPIN 1–127. Data were recorded for three different concentrations (20, 40, and 80 μM) at four velocities (18,000 rpm (○) bottom curve, 20,000 rpm (□), 26,000 rpm (△), and 30,000 rpm (▽) top curve and fitted to a monomer-dimer equilibrium model, which resulted in a K_d value of 160 μM.

domains covering residues 219–377 (Fig. 1*A*). In contrast, a scan of the region N-terminal to the UBL-NZF module against the PROSITE and SMART databases (18, 19) did not provide any hits for recognizable domains. Therefore, to gain three-dimensional insight into the N-terminal half of SHARPIN, we screened this region for soluble constructs of bacterially expressed fragments suitable for structural studies. One of the constructs that could be purified to homogeneity covers amino acids 1–127. This construct includes the region spanning amino acids 36–49 that displays a heptad repeat motif and is predicted with high propensity to form a short coiled coil. To investigate whether SHARPIN 1–127 indeed reversibly self-associates in solution, we performed sedimentation velocity experiments. At a concentration of 38 μM, the polypeptide primarily exists as a single species with a sedimentation coefficient of 1.3 S, which corresponds to a molecular mass of 13,150 Da, the mass of a SHARPIN monomer (Fig. 1*B*). However, when the SHARPIN concentration was increased by 2- and 4-fold, respectively, another species with a sedimentation coefficient of 1.9 S became apparent (Fig. 1*B*). This population corresponds to the molecular mass of a dimer, demonstrating that SHARPIN 1–127 exists in monomer-dimer equilibrium. The high concentrations required to form the dimeric species indicated a rather weak intermolecular interaction, and we were able to derive a dissociation constant of 160 μM by sedimentation equilibrium measurements (Fig. 1*C*). In an alternative approach, we determined the dissociation constant for the monomer-dimer equilibrium by isothermal titration calorime-

Downloaded from www.jbc.org at Frankfurt University Library / Section Bibliothek Naturwissenschaften, on August 31, 2012

TABLE 1
Statistics of data collection, phasing, and refinement
FOM, figure of merit.

Data collection	
Wavelength (Å)	0.9799
Resolution (Å)	30-2.0 (2.09-2.00)[a]
Space group	$P4_32_12$
Unit cell parameters (Å)	$a/b = 61.55$, $c = 222.81$
Total measurements	213,897
Unique reflections	55,100[b]
Average redundancy	3.9 (3.8)
I/σ	17.2 (2.9)
Completeness (%)	99.1
R_{merge} (%)[c]	7.1 (48.3)
Phasing	
No. of sites	2
Mean FOM (phaser) (30-2.6 Å)	0.53
No. of copies in the AU	4
Mean FOM (resolve) (30-2.4 Å)	0.73
Refinement	
Resolution (Å)	30-2.0
R_{work} (%)[d]	20.9
R_{free} (%)[e]	26.9
No. of atoms	3186
Protein	3186
Water	86
Average B-factor (Å^2)	34.5
r.m.s.d. from ideal values[f]	
Bond length (Å)	0.018
Bond angles	2.135°
Ramachandran plot	
Residues in most favored region (%)	96.0
Residues in additional allowed regions (%)	4.0

[a] Values in parentheses correspond to the highest resolution shell.
[b] Friedel pairs are treated as separate reflections.
[c] $R_{merge}(I) = \Sigma_{hkl}\Sigma_i|I_{hkl,i} - \langle I_{hkl}\rangle|/\Sigma_{hkl}\Sigma_i I_{hkl,i}|$, where $\langle I_{hkl}\rangle$ is the average intensity of multiple $I_{hkl,i}$ observations for symmetry-related reflections.
[d] $R_{work} = \Sigma_{hkl}|F_o - F_c|/\Sigma_{hkl}|F_o|$, where F_o and F_c are the observed and calculated structure factors, respectively.
[e] $R_{free} = \Sigma_{hkl}|F_o - F_c|/\Sigma_{hkl}|F_o|$ was calculated with 5% of the data omitted from structure refinement.
[f] r.m.s.d. represents root mean square deviation.

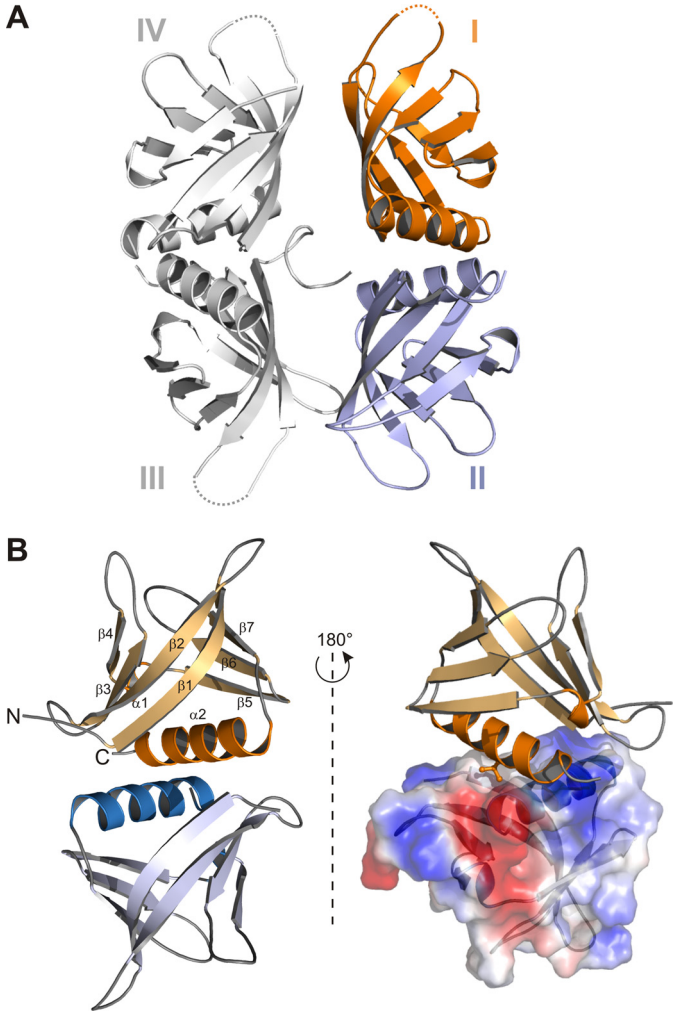

FIGURE 2. *A*, schematic presentation of all four PH domains observed in the asymmetric unit of the SHARPIN crystals. The loop region connecting strand β_1 with β_2 of subunits *I*, *III*, and *IV* are not observed in the density and indicated with *dashed lines*. *B*, overall structure shown as a *ribbon* representation of the non-crystallographic dimer of the SHARPIN PH domain. The electrostatic potential is projected on the surface of one subunit of the PH dimer. Valine 114 of the other subunit is depicted as *ball-and-stick* representation and points against the hydrophobic patch of the dimer interface. The structure is rotated by 180° with respect to the structure on the *left*.

try (ITC), which resulted in an ~2-fold lower K_d value of 88 μM. These data are consistent with the observation that SHARPIN multimerizes through its N-terminal region *in vivo* (1) and are the first molecular description of this self-association process.

N-terminal Region of SHARPIN Adopts PH Superfold—To understand the structural basis of SHARPIN dimerization, we crystallized the fragment containing residues 1–127. Crystals of space group $P4_32_12$ were grown in 4 M sodium formate from selenomethionine-derivatized protein, which diffracted to a maximal resolution of 2.0 Å with four molecules in the asymmetric unit. The structure was solved by single anomalous dispersion (Table 1 and supplemental Fig. S1). Remarkably, the structure of the four subunits in the asymmetric unit revealed that SHARPIN utilizes a PH fold for self-association (Fig. 2, *A* and *B*). Residues 20–120 of SHARPIN cover the canonical PH fold, which is a seven-stranded antiparallel β-sheet, strongly bent to form a β-barrel-like conformation and capped by a C-terminal α-helix. A helical turn that connects strand β4 and β5 of the collapsed β-barrel is the only variation of the conserved PH domain organization. Residues 1–20 adopt different conformations in the four copies in the asymmetric unit. The N terminus of one of the subunits is buried into the center of the symmetry axis of the tetramer and participates in intermolecular interactions with the other PH-like domains (Fig. 2*A*). The amino-terminal stretch of the diagonally opposite subunit makes contacts to symmetry related molecules. No density can be observed for the remaining other two N termini, indicating that they are disordered. Each of the protomers in the crystallographic tetramer forms two distinctive interfaces. Because our solution studies did not give any indication that SHARPIN assembles into higher order oligomers, it is likely that tetramerization is due to crystal packing. The subunits I and II are aligned head-to-head against the subunits IV and III, respectively, with a rotation of 180° degrees (Fig. 2*A*). This orientation causes the formation of a histidine-stacking interaction, which is sandwiched between two salt bridges and probably based on crystal contacts (supplemental Fig. S2). In comparison, the second interface (I–II and III–IV) (Fig. 2*B*) is formed predominantly by a perpendicular arrangement of the helical elements of two neighboring PH-like domains and involves the interplay of many more side chains (Fig. 3, *A* and *B*). Val-114 is in the center of a hydrophobic interface formed by Leu-115, Leu-21, and Phe-56 of the other dimer half (Fig. 3, *A* and *B*). The hydrophobic patch is limited by electrostatic interactions, which

Downloaded from www.jbc.org at Frankfurt University Library / Section Bibliothek Naturwissenschaften, on August 31, 2012

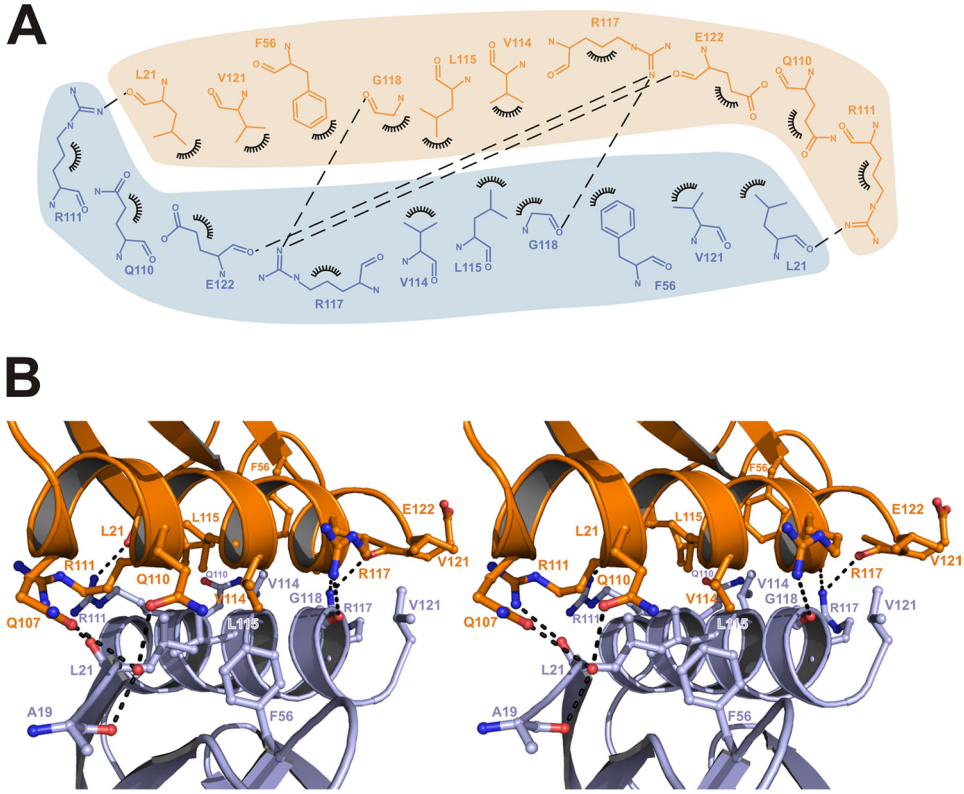

FIGURE 3. *A*, schematic drawing of interacting residues observed in the dimer interface. Hydrogen bonds (cutoff level of 3.5 Å) are shown as *dashed lines*. Hydrophobic interactions (cutoff level of 4.0 Å) are marked by *black eyelashes*. *B*, stereo view of the SHARPIN dimer interface. Residues participating in dimer formation are shown as *ball-and-sticks*.

involve the side chains of two arginines positioned at the C-terminal α-helix. Arg-111 binds the backbone oxygen of Leu-21 in β1 and Arg-117 coordinates the carbonyl group of Gly-118 and the side chain of Glu-122, which are both located at the tip of the helix. To confirm the relevance of the observed interface for self-association, we introduced a negative charge into the hydrophobic patch of the dimerization side. The mutation V114D should impair the hydrophobic network of the dimer interface and abolish dimerization in solution if this was the physiologically relevant dimer interface. In a complementary approach to our AUC analysis, we performed size exclusion chromatography coupled to multi-angle light scattering measurements of the wild-type and mutant PH-like domain. In these experiments, the retention time of wild-type SHARPIN shifts from a monomeric to a dimeric species when the concentration is increased in line with a monomer-dimer equilibrium (Fig. 4*A*). In contrast, the V114D mutant elutes as a monomer even at the very high concentration of 2.5 mM. Similarly, no monomer-dimer equilibrium can be observed for V114D when probed by ITC (Fig. 4*B*). These results clearly indicate that complex formation of the PH-like dimer is indeed formed via the helical interface observed in the crystal structure.

Does N-terminal Portion of SHARPIN Act as Protein Interaction Domain?—The PH superfold is a stable fold that has been adopted by a number of protein interaction domains that otherwise share no sequence homology but use the PH superfold as a scaffold upon which different ligand binding surfaces are crafted (20). These include PH domains themselves, which have been identified as phosphatidylinositol phosphate binding modules and function as membrane-targeting domains (21), as well as for example EVH1 (Enabled/VASP homology) domains, which act as protein-protein interaction modules (22, 23). Interestingly, only ~15% of all PH domains show specific lipid binding properties (21), whereas the majority bind phospholipid ligands only with low affinity and specificity or show no interaction at all. SHARPIN appears to belong to the latter group as it did not show any detectable phospholipid binding in protein lipid overlay assays (PIP strips, data not shown). In concordance, SHARPIN lacks the electrostatic polarization typically observed for those PH domains that bind to phospholipids and associate with negatively charged membrane surfaces (20) (supplemental Fig. S3, *A* and *B*), further supporting the notion that its PH-like domain most likely does not function as a lipid-binding module.

A search of the proteins structure database server DaliLite (version 3) (24) with our structure revealed the EVH1 (Enabled/VASP homology 1) domain of the scaffold protein HOMER as a close three-dimensional neighbor of SHARPIN (root mean square deviation, 2.6 Å^2) (25) (supplemental Fig. S4*A*). EVH1 domains adopt the same core structure as the PH domain and act as protein interaction modules via the recognition of polyproline-containing sequences (22, 23). However, despite the high structural similarity between SHARPIN and the EVH1 domain of HOMER, interaction of SHARPIN with proline-rich sequences is unlikely because SHARPIN lacks a highly conserved cluster of three surface-exposed aromatic amino acids that form the ligand binding site in EVH1 domains (supplemental Fig. S4*B*). Indeed, when we tested the ability of SHARPIN to

Downloaded from www.jbc.org at Frankfurt University Library / Section Bibliothek Naturwissenschaften, on August 31, 2012

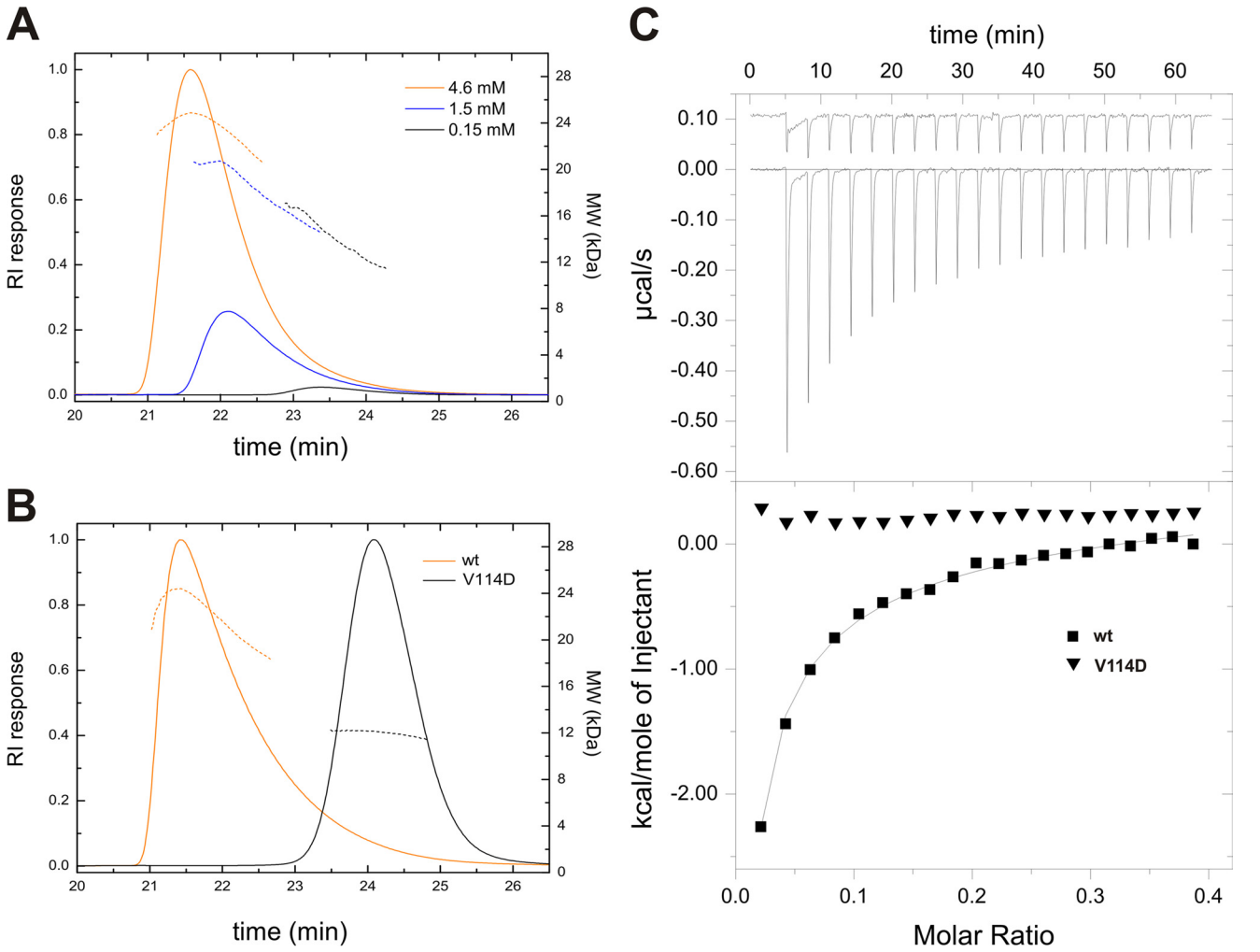

FIGURE 4. *A*, size exclusion chromatography-MALS measurements of SHARPIN 1–127 at three different concentrations (0.15, 1.5, and 4.6 mM). The molecular mass (*MW*) distributions of the eluent are shown as *dashed lines* and the refractive index (*RI*) response is shown as a solid line. *B*, comparison of size exclusion chromatography-MALS analysis of SHARPIN 1–127 WT and V114D. Both measurements were performed at a molar concentration of 2.5 mM. *C*, dimer dissociation probed by ITC. 1 mM SHARPIN PH domain WT or V114D was injected into the calorimeter cell containing buffer, and dissociation thermograms were recorded. The fitted data yield the equilibrium dissociation constant for wild-type SHARPIN of 88 μM.

bind peptides derived from classical EVH1 domain ligands using ITC, we could not detect any interaction (data not shown). Furthermore, a yeast two-hybrid screen using the N-terminal 127 amino acids as a bait to identify novel protein partners of the PH domain of SHARPIN did not yield any hits.

Based on these observations, we suggest that in SHARPIN, the PH domain is not used as a protein-ligand interaction platform but rather a scaffold that provides the structural basis for homodimerization that occurs under *in vitro* conditions as shown by our MALS, AUC, and ITC experiments and *in vivo* (1). The crystal structure of the SHARPIN PH domain reveals that the dimer is formed primarily by hydrophobic interactions between two helices, which are packed head-to-head in an almost rectangular manner. The interface area covers a solvent accessible surface area of 616 Å^2 (26). A binding site of this magnitude is often characteristic for moderate to weak protein-protein interactions and therefore in good agreement with the experimental binding constant of 88 and 160 μM determined by ITC and AUC, respectively (27). Despite the high K_d value determined for PH domain dimerization, the interaction is highly specific. Incorporation of a single electrostatic charge in the center of the hydrophobic framework of the interface by mutating Val-114 to Asp completely abolishes interaction. The fact that SHARPIN dimerization is mediated by a PH domain and not as originally assumed by a predicted coiled coil was unexpected and somewhat surprising. However, in this context, it is interesting to note that dimer formation of proteins mediated by the PH superfold has been suggested before, although the phenomenon has not been investigated on a molecular level. The activity of phosphoinositide-dependent kinase 1 for instance is dependent on 3-phosphoinositide-dependent homodimerization of its C-terminal PH domain (28). Similarly, it has been reported that the PH domain of dynamin undergoes a phosphoinositide binding-coupled monomer-dimer equilibrium (29, 30). Although in both of these cases, PH domain-mediated dimerization is coupled to the interaction with lipids, it raises the possibility that self-association via PH domains is a more general function for the PH superfold.

In conclusion, the structure of the N-terminal portion of SHARPIN presented here shows that it adopts the PH domain superfold. Our data suggest that, unlike what is generally assumed this domain does not act as a protein interaction mod-

Downloaded from www.jbc.org at Frankfurt University Library / Section Bibliothek Naturwissenschaften, on August 31, 2012

ule but as a dimerization domain, thereby extending the manner in which the PH fold can be used as a protein scaffold. Current data suggest that this region does not contribute to the catalytic activity of LUBAC (5),[3] indicating that it may play a role in other physiological functions of SHARPIN that have been described, such as its tumor-associated role or its ability to inhibit β1-integrin activation (1, 31–33). Further studies are required to better understand these functions and to test whether self-association might be a regulated process.

Acknowledgments—We are grateful to Philip Walker for data collection and David Goldstone for assistance with analytical ultracentrifugation. We thank Vanja Nagy, Sigrid Skånland, and Jaime Lopez-Mosgueda for help with reagents and insightful discussions.

REFERENCES

1. Lim, S., Sala, C., Yoon, J., Park, S., Kuroda, S., Sheng, M., and Kim, E. (2001) Sharpin, a novel postsynaptic density protein that directly interacts with the shank family of proteins. *Mol. Cell Neurosci.* **17,** 385–397
2. Seymour, R. E., Hasham, M. G., Cox, G. A., Shultz, L. D., Hogenesch, H., Roopenian, D. C., and Sundberg, J. P. (2007) Spontaneous mutations in the mouse Sharpin gene result in multiorgan inflammation, immune system dysregulation and dermatitis. *Genes Immun.* **8,** 416–421
3. Ikeda, F., Deribe, Y. L., Skånland, S. S., Stieglitz, B., Grabbe, C., Franz-Wachtel, M., van Wijk, S. J., Goswami, P., Nagy, V., Terzic, J., Tokunaga, F., Androulidaki, A., Nakagawa, T., Pasparakis, M., Iwai, K., Sundberg, J. P., Schaefer, L., Rittinger, K., Macek, B., and Dikic, I. (2011) SHARPIN forms a linear ubiquitin ligase complex regulating NF-κB activity and apoptosis. *Nature* **471,** 637–641
4. Gerlach, B., Cordier, S. M., Schmukle, A. C., Emmerich, C. H., Rieser, E., Haas, T. L., Webb, A. I., Rickard, J. A., Anderton, H., Wong, W. W., Nachbur, U., Gangoda, L., Warnken, U., Purcell, A. W., Silke, J., and Walczak, H. (2011) Linear ubiquitination prevents inflammation and regulates immune signaling. *Nature* **471,** 591–596
5. Tokunaga, F., Nakagawa, T., Nakahara, M., Saeki, Y., Taniguchi, M., Sakata, S., Tanaka, K., Nakano, H., and Iwai, K. (2011) SHARPIN is a component of the NF-κB-activating linear ubiquitin chain assembly complex. *Nature* **471,** 633–636
6. Eisenhaber, B., Chumak, N., Eisenhaber, F., and Hauser, M. T. (2007) The ring between ring fingers (RBR) protein family. *Genome Biol.* **8,** 209
7. Kirisako, T., Kamei, K., Murata, S., Kato, M., Fukumoto, H., Kanie, M., Sano, S., Tokunaga, F., Tanaka, K., and Iwai, K. (2006) A ubiquitin ligase complex assembles linear polyubiquitin chains. *EMBO J.* **25,** 4877–4887
8. Tokunaga, F., Sakata, S., Saeki, Y., Satomi, Y., Kirisako, T., Kamei, K., Nakagawa, T., Kato, M., Murata, S., Yamaoka, S., Yamamoto, M., Akira, S., Takao, T., Tanaka, K., and Iwai, K. (2009) Involvement of linear polyubiquitylation of NEMO in NF-κB activation. *Nat. Cell Biol.* **11,** 123–132
9. Iwai, K., and Tokunaga, F. (2009) Linear polyubiquitination: A new regulator of NF-κB activation. *EMBO Rep.* **10,** 706–713
10. Emmerich, C. H., Schmukle, A. C., and Walczak, H. (2011) The emerging role of linear ubiquitination in cell signaling. *Sci. Signal.* **4,** re5
11. Otwinowski, Z., and Minor, W. (1996) Processing of X-ray diffraction data collected in oscillation mode. *Methods in Enzymology* **276,** 307–326
12. Adams, P. D., Afonine, P. V., Bunkóczi, G., Chen, V. B., Davis, I. W., Echols, N., Headd, J. J., Hung, L. W., Kapral, G. J., Grosse-Kunstleve, R. W., McCoy, A. J., Moriarty, N. W., Oeffner, R., Read, R. J., Richardson, D. C., Richardson, J. S., Terwilliger, T. C., and Zwart, P. H. (2010) PHENIX: A comprehensive Python-based system for macromolecular structure solution. *Acta Crystallogr. D Biol. Crystallogr.* **66,** 213–221
13. Emsley, P., and Cowtan, K. (2004) Coot: Model-building tools for molecular graphics. *Acta Crystallogr. D Biol. Crystallogr.* **60,** 2126–2132
14. Murshudov, G. N., Vagin, A. A., and Dodson, E. J. (1997) Refinement of macromolecular structures by the maximum likelihood method. *Acta Crystallogr. D Biol. Crystallogr.* **53,** 240–255
15. Laskowski, R. A., Moss, D. S., and Thornton, J. M. (1993) Main-chain bond lengths and bond angles in protein structures. *J. Mol. Biol.* **231,** 1049–1067
16. Schuck, P. (2000) Size distribution analysis of macromolecules by sedimentation velocity ultracentrifugation and lamm equation modeling. *Biophys. J.* **78,** 1606–1619
17. Schuck, P. (2003) On the analysis of protein self-association by sedimentation velocity analytical ultracentrifugation. *Anal. Biochem.* **320,** 104–124
18. Letunic, I., Doerks, T., and Bork, P. (2009) SMART 6: Recent updates and new developments. *Nucleic Acids Res.* **37,** D229–232
19. Hulo, N., Bairoch, A., Bulliard, V., Cerutti, L., De Castro, E., Langendijk-Genevaux, P. S., Pagni, M., and Sigrist, C. J. (2006) The PROSITE database. *Nucleic Acids Res.* **34,** D227–230
20. Blomberg, N., Baraldi, E., Nilges, M., and Saraste, M. (1999) The PH superfold: A structural scaffold for multiple functions. *Trends Biochem. Sci.* **24,** 441–445
21. Lemmon, M. A., and Ferguson, K. M. (2000) Signal-dependent membrane targeting by pleckstrin homology (PH) domains. *Biochem. J.* **350,** 1–18
22. Ball, L. J., Jarchau, T., Oschkinat, H., and Walter, U. (2002) EVH1 domains: Structure, function, and interactions. *FEBS Lett.* **513,** 45–52
23. Peterson, F. C., and Volkman, B. F. (2009) Diversity of polyproline recognition by EVH1 domains. *Front Biosci.* **14,** 833–846
24. Holm, L., and Park, J. (2000) DaliLite workbench for protein structure comparison. *Bioinformatics* **16,** 566–567
25. Beneken, J., Tu, J. C., Xiao, B., Nuriya, M., Yuan, J. P., Worley, P. F., and Leahy, D. J. (2000) Structure of the Homer EVH1 domain-peptide complex reveals a new twist in polyproline recognition. *Neuron* **26,** 143–154
26. Jones, S., and Thornton, J. M. (1996) Principles of protein-protein interactions. *Proc. Natl. Acad. Sci. U.S.A.* **93,** 13–20
27. Nooren, I. M., and Thornton, J. M. (2003) Diversity of protein-protein interactions. *EMBO J.* **22,** 3486–3492
28. Masters, T. A., Calleja, V., Armoogum, D. A., Marsh, R. J., Applebee, C. J., Laguerre, M., Bain, A. J., and Larijani, B. (2010) Regulation of 3-phosphoinositide-dependent protein kinase 1 activity by homodimerization in live cells. *Sci. Signal.* **3,** ra78
29. Klein, D. E., Lee, A., Frank, D. W., Marks, M. S., and Lemmon, M. A. (1998) The pleckstrin homology domains of dynamin isoforms require oligomerization for high affinity phosphoinositide binding. *J. Biol. Chem.* **273,** 27725–27733
30. Fushman, D., Cahill, S., Lemmon, M. A., Schlessinger, J., and Cowburn, D. (1995) Solution structure of pleckstrin homology domain of dynamin by heteronuclear NMR spectroscopy. *Proc. Natl. Acad. Sci. U.S.A.* **92,** 816–820
31. Jung, J., Kim, J. M., Park, B., Cheon, Y., Lee, B., Choo, S. H., Koh, S. S., and Lee, S. (2010) Newly identified tumor-associated role of human Sharpin. *Mol. Cell Biochem.* **340,** 161–167
32. Landgraf, K., Bollig, F., Trowe, M. O., Besenbeck, B., Ebert, C., Kruspe, D., Kispert, A., Hänel, F., and Englert, C. (2010) Sipl1 and Rbck1 are novel Eya1-binding proteins with a role in craniofacial development. *Mol. Cell. Biol.* **30,** 5764–5775
33. Rantala, J. K., Pouwels, J., Pellinen, T., Veltel, S., Laasola, P., Mattila, E., Potter, C. S., Duffy, T., Sundberg, J. P., Kallioniemi, O., Askari, J. A., Humphries, M. J., Parsons, M., Salmi, M., and Ivaska, J. (2011) SHARPIN is an endogenous inhibitor of β1-integrin activation. *Nat. Cell Biol.* **13,** 1315–1324

[3] B. Stieglitz, unpublished observations.

Downloaded from www.jbc.org at Frankfurt University Library / Section Bibliothek Naturwissenschaften, on August 31, 2012